ISSN 1946-7664. MCFNS 2020
Vol. 12, Issue 1, pp. 26–49
Mathematical and Computational Forestry & Natural-Resource Sciences

AVAILABLE ONLINE AT HTTP://MCFNS.COM

Submitted: Oct. 3, 2019
Accepted: Feb. 26, 2020
Published: Mar. 30, 2020
Last Correction: Mar. 30, 2020

CROWN ASYMMETRY AND NICHE SEGREGATION AS AN ADAPTATION OF TREES TO COMPETITION FOR LIGHT: CONCLUSIONS FROM SIMULATION EXPERIMENTS IN MIXED BOREAL STANDS

V. Shanin[1,2,3] , P. Grabarnik[1] , M. Shashkov[1,3] , N. Ivanova[1,3] , S. Bykhovets[1] , P. Frolov[1] , M. Stamenov[1]

[1] *Institute of Physicochemical and Biological Problems in Soil Science of the Russian Academy of Sciences, Pushchino, Russian Federation*
[2] *Center for Forest Ecology and Productivity of the Russian Academy of Sciences, Moscow, Russian Federation*
[3] *Institute of Mathematical Problems of Biology – the Branch of the Keldysh Institute of Applied Mathematics of the Russian Academy of Sciences, Pushchino, Russian Federation*

Abstract. Most models of forest communities cannot represent the asymmetry of crowns resulting from inter-tree competition. However, such a representation is important for the accurate simulation of mixed and uneven-aged forest stands. In the paper we propose a new model of a forest stand, which is individual-based and spatially-explicit, i.e., taking into account the relative positions and properties of all competing trees within a plot. The model uses species-specific coefficients to take into account the different strategies of competition for light. The model operates with the 3D-representation of tree crowns and light transmission through the canopy using discrete spatial and temporal resolution. It is thus capable to represent the asymmetry of crown shapes and biomass distribution being a response of tree geometry to the local surrounding of the given tree. In order to estimate the performance of the model in the simulation of aboveground competition, a set of simulation scenarios, representing stands of different spatial structures, ages, and species compositions, were used. Simulations showed a positive effect of species mixture on crown size and light interception efficiency, as well as species- and age-related dependencies of these parameters. Differences in the spatial structure mostly affected the light transmission pattern at the stand level. The importance of crown asymmetry in the increase of light interception efficiency was also shown. Thus, the proposed model allows to simulate light absorption by the canopy with a high spatial resolution, using relatively few parameters. The model imitates a mechanism allowing trees to decrease the aboveground competition in forest stands, and it is also applicable for simulating aboveground competition in mixed uneven-aged stands.

Keywords: Competition; PAR; crown asymmetry; mixed uneven-aged stands; wood quality.

1 BACKGROUND

The spatial structure of forest stands, which emerges from the location of individual trees, their sizes, and the shapes of their below- and above-ground organs, is usually heterogeneous and represents an assemblage of trees irregularly located and remarkably different in size and shape. Over time, the spatial structure can vary as result of changes in species composition and age structure, the strength of competition between trees, and the frequency and intensity of various disturbances. During stand development, the spatial structure changes occur not only due to self-thinning, but also because of changes in the size and shape of individual tree crowns. The latter is a result of the predominant growth of branches under favorable light conditions and of the dieback of shaded parts of the crown. Asymmetric crowns, with different widths in different horizontal directions, are formed as a result of this process. Thus, local interactions among individuals are a substantial factor for the formation of plant communities (Green, Sadedin, 2005; Uria-Diez, Pommerening, 2017). For example, studies in beech forests of Germany have shown significant differences

in annual length growth among branches growing towards the canopy gaps (9.2 $cm \cdot yr^{-1}$) and other branches (6.2 $cm \cdot yr^{-1}$) (Haywood, 2002). Similar trends have been found for pine on dried peatlands of north-eastern Switzerland (Stoll, Schmid, 1998). Such an adaptation mechanism to competition through asymmetric crown expansion in different directions promotes a more efficient interception of photosynthetically active radiation (PAR) at the community, not individual, level, resulting in a higher stand productivity (Danilov, Ishchuk, 2013). This effect is most noticeable in mixed stands, where the co-existence of trees of different species allows for a more efficient allocation of their photosynthesizing organs. Generally, this results in a higher productivity of mixed stands in comparison to pure ones (Morin et al., 2011; Pretzsch, 2014; Pretzsch, Schütze, 2016). There are several studies of the spatial structure of stands and its relationship with the asymmetry of individual crowns (e.g., Brisson, 2001; Rouvinen, Kuuluvainen, 1997; Schröter et al., 2012).

Most forest community models are unable to represent the asymmetry of crowns resulting from inter-tree competition, although this is an important factor (Cescatti, 1997a). The underestimation of crown plasticity in simulation models may lead to an incorrect estimation (to either under- or overestimation) of competition intensity in different parts of the canopy and, as a result, to errors in the calculation of biomass production of individual trees.

The simplest and most common approach to simulate competition in plant communities is the use of competition indices as proxies for the intensity and direction of interactions between individual plants (Daniels et al., 1986). Further development of competition models use the ecological field theory (Wu et al., 1985), which was applied in the description of interactions between trees in individual-based models (Seidl et al., 2012; García, 2014; Yeatts, 2012). However, competition indices usually do not take into account the differences between above- and belowground competition (e.g., size-symmetry, resource exhaustibility, etc.).

So far, numerous models of aboveground competition have been developed. The simplest ones consider competition as the overlapping of flat and horizontally oriented "shadowing zones" of trees, while more complex models use the 3-dimensional representation of crowns, with accurate calculation of solar radiation transmission through the canopy. Some of the models use the exact representation of crown architecture (Renshaw, 1985; Perttunen, 2009), although they are unable to accurately take into account the influence of competition from neighboring trees on crown formation. The main shortcomings of most of the existing models of aboveground competition are: (i) neglecting the heterogeneity of biomass distribution inside the crown and (ii) representation of crowns as figures centrally symmetrical on their vertical axis, without taking into account the asymmetry resulting from competition. Some of the models are able to simulate asymmetry (Cescatti, 1997a,b; Lebedev, Chumachenko, 2011; Kędra, Gazda, 2016), but it is usually assigned in such models using an external parameters rather than calculated dynamically from the data on surrounding of given tree. Two models taking into account the heterogeneity of biomass distribution inside the crown are Mixfor-3D (Olchev et al., 2009) and PIXTA (Lebedev, Chumachenko, 2011). In PIXTA the spatial inhomogeneity of the incoming light regime is the determinant factor of unequal crown expansion in different directions. Notably, the light regime sub-model is able to define the inhomogeneity in filling the crown volume by phytoelements (Lebedev, Chumachenko, 2002). However, the approach assuming the simplification of the models which involves the representation of a vertical stand structure as a set of several layers is still popular (e.g. Collalti et al., 2014; Kolobov, Frisman, 2016).

In view of the strengths and weaknesses of the existing models, a new model of aboveground competition between trees presented here, has emphasis on the asymmetry of crown shape and biomass distribution in response to competition in mixed and uneven-aged stands. The model is intended to be included into the ecosystem model (Komarov et al., 2003) which is used for the assessment of population dynamics and the biological turnover of carbon and nitrogen in mixed, uneven-aged boreal forest stands. The species-specific model parameters were estimated for Scots pine (*Pinus sylvestris* L.), Norway spruce (*Picea abies* (L.) H. Karst.), and birch (the same parameters were set for both *Betula pendula* Roth and *Betula pubescens* Ehrh.). The general objectives of the paper are (i) to describe the structure of the model, with special emphasis on its features related to the simulation of crown asymmetry; (ii) describe the parameterization, verification and sensitivity analysis of the model; and (iii) show the performance of the model with simulations across forest stands with contrasting structure.

2 MATERIALS AND METHODS

2.1 General Description of the Model

The suggested model describes the competition between trees for PAR. The model is individual-based and spatially-explicit, i.e., it takes into account the relative positions and properties of all competing trees in a forest stand.

The simulation plot is divided into 3D cells, represented as rectangular prisms with a base size of 0.5 × 0.5

m and a height of 1 m. The crowns of all trees are approximated by such cells, and each cell may contain crowns of several trees. The size of the cell base was chosen to be equal to the most typical cell size in the ecosystem model EFIMOD (Komarov et al., 2003). The model requires the following input data: spatial location, species, age, height, and stem diameter at breast height for each individual tree. The outputs of the model are the amount of PAR absorbed by each tree and the spatial distribution of PAR intensity below the canopy. The model is dynamic and is able to reproduce the changes of crown shapes of individual trees over time resulted from the competition. The basic time step (described below) is 1 year while some sub-routines have smaller time step.

2.2 Calculation of Crown Size

Crown size is defined by (i) total tree height, (ii) height of crown base, and (iii) maximum crown width. The crown is represented by one of axisymmetric bodies: cylinder, vertically-asymmetric ellipsoid, semi-ellipsoid, composite cone, and upside-down cone. The basic crown shape is a species-specific feature: for pine, the vertically-asymmetric ellipsoid is used, while for spruce, the composite cone and for birch, the semi-ellipsoid are used. Crown shapes are based on basic shapes presented in some previous works (e.g., Pretzsch et al., 2002; Widlowski et al., 2003), with additional improvements (Figure 1).

The equations for the calculation of basic crown dimensions were adopted from (Thorpe et al., 2010) and

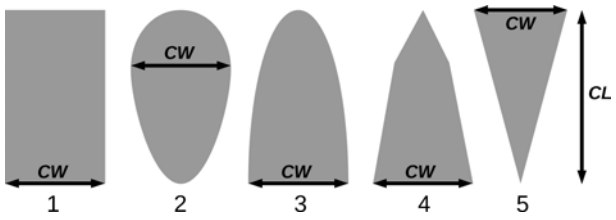

Figure 1: Planar figures, generating axisymmetric bodies for the representation of species-specific crown shapes: 1 - cylinder (the shape is reserved), 2 - vertically-asymmetric ellipsoid (pine), 3 - semi-ellipsoid (birch), 4 - composite cone (spruce), 5 - upside-down cone (reserved). Dimension CW denotes maximum crown width, i.e., crown width in its widest part (double maximum crown radius), dimension CL denotes crown length in the vertical direction (total tree height minus crown base height).

use tree height, stem diameter at breast height (DBH), and local competition indices as predictor variables.

$$CR = \nu_{CR} \cdot \left(1 - e^{\eta_{CR} \cdot DBH}\right) \cdot e^{\kappa_{CR} \cdot NCI}, \qquad (1)$$

$$CL = \nu_{CL} \cdot \left(1 - e^{\eta_{CL} \cdot H}\right) \cdot e^{\kappa_{CL} \cdot NCI}, \qquad (2)$$

where CR is the maximum crown radius, CL is the crown length, NCI is the competition index representing local stand density around the given tree (see below), ν, η, and κ are empirical coefficients (index $_{CR}$ denotes crown radius, and index $_{CL}$ denotes crown length). Thus, competition strength (expressed though the local stand density) affects crown size. Crown length is considered as total tree height minus crown base height.

The influences of all trees ($j = 1, 2, \ldots, n$) of different species ($i = 1, 2, \ldots, s$) closer than 10 m to the focal tree were taken into account when calculating the competition indices. The "complete model" takes into account the decrease in competitive pressure from neighbors with increasing size of the focal tree:

$$NCI_t^{DBH} = \sum_{i=1}^{s} \sum_{j=1}^{n} \left(\frac{\mu_t}{\mu_i}\right) \cdot \frac{DBH_{ij}^{\alpha}}{l_{ij}^{\epsilon}} \cdot e^{\gamma \cdot DBH_t}, \qquad (3)$$

$$NCI_t^{H} = \sum_{i=1}^{s} \sum_{j=1}^{n} \left(\frac{\mu_t}{\mu_i}\right) \cdot \frac{H_{ij}^{\alpha}}{l_{ij}^{\epsilon}} \cdot e^{\gamma \cdot H_t}, \qquad (4)$$

where l_{ij} is the distance between focal and competing tree, DBH_{ij} and H_{ij} are stem diameter at breast height and total height, respectively, of the competing tree, DBH_t and H_t are stem diameter at breast height and total height, respectively, of the focal tree (t), α, ε, γ, μ are species-specific coefficients (Thorpe et al., 2010). Coefficients of Equations (1–4) were estimated with published data (Pugachevskiy, 1992; Rautiainen, Stenberg, 2005; Tahvanainen, Forss, 2008; Tselniker et al., 1999; Usoltsev, 2013b, 2016a; Widlowski et al., 2003) on crown sizes for stands of different structure and composition using the least squares method (more details in Appendix A).

The resulting 3D objects describing crown shape and size of individual trees are divided into horizontal layers with an interval of 1 m. If the crown does not occupy the whole layer in a vertical direction (which is possible for undermost and uppermost of layers to which the crown is expanded), the model accepts, during approximation, that the crown is presented in the given layer if it occupies more than half of the layer's height. To avoid cases where the crown is not presented in any layer, for trees whose crowns occupy less than half of any layer in a vertical direction, the model accepts that the crown is presented in the layer in which its extension in the vertical direction is maximal. Then basic crown radius

in each layer is calculated as the radius of the axisymmetric body representing basic crown shape at relative height corresponding to the midpoint of the given layer. Inside the layer, the crown is approximated by rectangular prisms with a typical base size of 0.5 × 0.5 m and a height of 1 m.

2.3 Construction of Actual Crown Shape

To modify crown radius as result of the competitive pressure from neighboring trees, the potential areas for crown expansion should be determined for each tree. This step assumes the partitioning of the simulation plot into subsets of cells, where each cell in such subset is closer to the given tree than to other trees (i.e., spatially-discrete implementation of Voronoi partitioning (Iles, 2009; Tran et al., 2009)). Such subsets are built separately for each layer, and only trees whose crowns are presented in the given layer are taken into account in the partitioning. The amount of cells occupied by the crown of the tree is defined by the area of crown projection in a given layer, which is numerically equal to the area of the circle with a radius equal to the crown radius in this layer. To determine the actual crown shape in each layer, the algorithm adds cells to the crown area, starting from those closest to the stem, according to the following empirical rules: (i) the cell from the potential crown area of the focal tree can be included into the crown if the horizontal distance between this cell and the rooting cell for the given tree is no more than 1.5 of the basic crown radii for a given layer (thus representing maximum possible extension of the crown), and (ii) the cell from the potential crown area of the neighboring tree can be included into the crown of the focal tree if the horizontal distance between this cell and the rooting cell for the focal tree is no more than 0.75 of the basic crown radii for a given layer (parameters E_{max} and E_{min}, respectively). The second rule has an additional species-specific modifier E_{corr}, whose values are set at 0.75, 1.25, and 1.00 for pine, spruce, and birch, respectively. The values of the modifiers were obtained from analysis of empirical data on asymmetry and overlapping of crown projections in mapped mixed forest stands on sampling plots (Shanin et al., 2016) and (due to high variability) rounded with a 0.25 discretization step. Some cells can be attributed to crowns of several trees. In such case the PAR between trees is distributed proportionally to the biomass of leaves / needles in given cell (see details below). The complete procedure is executed only at the initial step, while on further steps the algorithm only modifies crown size and shape according to changes of focal tree size and its environment.

2.4 Biomass Distribution Inside the Crown

In the following stage, the model distributes the biomass of photosynthesizing (leaves/needles) and non-photosynthesizing (stem and branches) organs among the cells composing the tree crown. The biomass values of different tree compartments are the output parameters of the productivity sub-model (Shanin et al., 2019) in the system of the models EFIMOD. The model takes into account the heterogeneity in both vertical and horizontal (from stem to the periphery of the crown and in different directions) distributions of biomass among cells, while the distribution of biomass inside the cell is assumed to be homogeneous. The structure of the model assumes that spatial asymmetry in the distribution of photosynthesizing organs inside the crown is mostly defined by the competition from neighboring trees rather than by other factors, such as species-specific featuRes. Such an approach, to our opinion, is simpler and more efficient in comparison to the approach using explicit ray-tracing, but with a simplified representation of crowns.

The vertical distribution of biomass is described as follows:

$$m_{cum} = \sigma + \tau \cdot \left(1 - e^{\psi \cdot H_{rel}}\right)^{\omega} \cdot \chi, \qquad (5)$$

where m_{cum} is the cumulative relative mass of the crown component (branches or foliage) in a given cell, H_{rel} is the relative height of a given point inside the crown (taking total crown length as 1), σ, τ, ψ, ω are the modifiers (Tahvanainen, Forss, 2008), and χ is the scaling factor to set the m_{cum} at 1 when H_{rel} is equal to 1. The previously estimated in (Tahvanainen, Forss, 2008) coefficients of equation were adjusted using an additional experimental data (Bobkova et al., 2000; Gspaltl et al., 2013; Gulbe et al., 1983; Mäkelä, Vanninen, 2001; Usoltsev, 2013a; Yarmishko, 1999) using the least squares method (more details in Appendix A). The vertical distribution of stem biomass is calculated based on the representation of the stem as a truncated cone, strictly circular at any horizontal section, with a radius of the upper circle set at 0.25 of the radius of the basal circle. Stem biomass in each layer is added to the biomass of the branches for the cell, which horizontal coordinates are the same as those of the stem base. The model first distributes biomass among the horizontal layers of an individual crown, according to Equation (5), and then calculates the biomass distribution among cells inside the given layer.

Since detailed data on the radial distribution of phytomass are lacking, the description of the radial distribution of biomass inside the crown layer is based on the assumption that leaf/needle biomass linearly increases from the crown center to the periphery and from northern to southern parts of an individual crown (Olchev et al., 2009). Similarly, the model assumes that

the mass of branches per cell linearly decreases from the stem center to the periphery. The differences in biomass distribution in cardinal directions is described with additional weighting factors A_N, A_E, A_S, and A_W, whose values are set at 0.9, 1.0, 1.1, and 1.0 for northern, eastern, southern, and western sectors of the crown, respectively (Olchev et al., 2009). The construction of the actual crown shape is schematically presented in Figure 2.

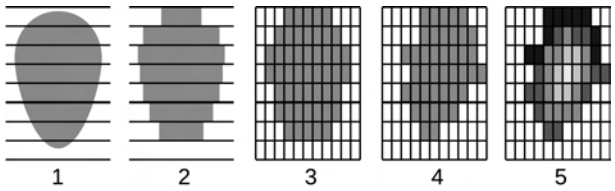

Figure 2: Schematic representation of the construction of actual crown shape (vertical cross-section aside on stem was taken as an example): 1 - basic crown shape; 2 - dividing of crown into horizontal layers, 3 - approximation of crown by 3D cells, 4 - modifying crown expansion in horizontal direction according to asymmetric competitive pressure from neighboring trees; 5 - distribution of aboveground biomass among cells.

2.5 Interception and Absorption of PAR

In this stage, the model describes the interception and absorption of PAR by tree crowns. If crowns of several trees are presented in a given cell, PAR is distributed among them proportionally to the leaf area density (LAD, $m^2 \cdot m^{-3}$) of competing trees in this cell (see details below).

Prior to the calculation of PAR interception/absorption, the biomass of leaves/needles in each 3D cell should be recalculated into LAD:

$$LAD = \frac{B_l \cdot S_{LV}}{V_{cell}}, \tag{6}$$

where B_l is the biomass of leaves/needles in a given cell (kg), S_{LV} is the species-specific single-sided leaf area ($m^2 \cdot kg^{-1}$) (Collalti et al., 2014; Gulbe et al., 1983; Ross, 1981; Widlowski et al., 2003), and V_{cell} is the cell volume (m^3).

The density of the PAR flux above the canopy at a clear sky is calculated according to (Peng et al., 2002). More details are provided in Appendix B. The amount of PAR is calculated with an hourly step, and subsequently, the sum of above-canopy PAR for the entire vegetation period (with a mean daily temperature above +5°C) is calculated. The amount of incoming PAR at actual cloudiness is reduced according to the assumption that the amount of PAR at cloudy sky comprises 0.2 of the PAR value at a clear sky:

$$\begin{aligned} PAR &= (1 - C_{cld}) \cdot PAR_0 + 0.2 \cdot C_{cld} \cdot PAR_0 \\ &= PAR_0 \cdot (1 - -0.8 \cdot C_{cld}), \end{aligned} \tag{7}$$

where C_{cld} is the coefficient to take into account the influence of cloudiness. For the central part of the East-European plain, the value of this coefficient was set to 0.42.

The model uses the simplified representation of the distribution of incoming solar radiation over the sky and the transmission of radiation through the forest canopy. The number of directions for incoming PAR was set to 5: one from the zenith and four from the cardinal directions (geographical north, south, east, and west). We assumed that scattered solar radiation is isotropic (i.e., its intensity is the same in all directions), while the income of direct solar radiation is distributed among eastern, southern, and western directions proportionally to the sums of the direct radiation for time intervals from dawn until 9.00, from 9.00 until 15.00, and from 15.00 until sunset, respectively. These sums (more specifically - their ratios) were estimated from the climate data sheets and the daily portions of direct and scattered solar radiation. For the central part of the East-European plain (Anonymous, 1987–2001), the sums of direct and scattered solar radiation at moderate cloudiness were assumed to be approximately equal (i.e. the portion of direct solar radiation, P_{dir}, was set at 0.5), and the ratio of above-mentioned "morning" (R_{mrn}), "afternoon" (R_{aft}), and "evening" (calculated as $1-R_{mrn}-R_{aft}$) sums of direct radiation was taken as 0.2:0.6:0.2. As a result, the portions of radiation from the zenith and from the north were set at 10% both, while from east and west, they were set at 20%, and from south at 40% of the total incoming solar radiation during the vegetation season. The elevation angle of the incoming solar beam of the scattered radiation from the northern direction was taken at 22°, and corresponding angles for the other directions were calculated taking into account the weighted average solar angle for the corresponding period and the ratio between direct and scattered radiation coming from the given direction.

The amount of absorbed PAR for each cell (i denotes the ordinal number of the given cell along the beam path) is calculated as follows:

$$APAR_i = PAR_i \cdot \left(1 - e^{-\rho \cdot LAD_i \cdot s_i}\right), \tag{8}$$

where PAR_i is the weighted average of incoming PAR intensity for a given direction ($MJ \cdot m^{-2} \cdot mo^{-1}$), which, in turn, is calculated as PAR transmitted through the previous cell along the beam path:

$$PAR_i = PAR_{i-1} \cdot e^{-\rho \cdot LAD_{i-1} \cdot s_{i-1}}, \tag{9}$$

and for the first cell along the beam path, the value of PAR_i is equal to the amount of PAR coming from the given direction; LAD is the leaf area density ($m^2 \cdot m^{-3}$), s_i is the length of the beam path in given cell, ρ is the empirical species-specific coefficient of solar radiation absorption (Aubin et al., 2000; Bossel, 1996; Duursma, Mäkelä, 2007; Lintunen et al., 2013). The amount of PAR absorbed in each cell is summed for all directions and, consequently, for all cells comprising the crown of a given tree.

The interception of PAR by non-photosynthesizing organs is assumed to be directly proportional to the share of the cell volume occupied by these organs. The model is based on the assumption that the portion of intercepted PAR linearly increases with the share of the cell volume occupied by the branches, reaching 1 at a share of 50% and higher. The volume of branches is calculated based on average wood density (Cieszewski et al., 2013; Repola, 2006). Due to the simplified representation of PAR interception in the current version of the model, an additional procedure was implemented, which simulates the horizontal light scattering resulting from multiple refraction and reflection inside the canopy. This procedure is based on the assumption that such scattering among neighboring cells comprises on average 10%. This allows the partial compensation of shortcomings of the existing ray-tracing algorithm, based on the limited number of discrete directions of incoming sunlight. If the values of PAR is lower than the species-specific threshold value L_{min} (in terms of portion of the PAR above the canopy), dieback of foliage in this cell is simulated (Evstigneev, 2018). The values of species-specific coefficients of the model are summarized in Appendix C.

3 RESULTS

3.1 Verification of the Model

The difficulty with the verification of such models is the absence of data from direct measurements of the amounts of PAR intercepted by individual trees, which is the basic output variable. However, some intermediate and collateral state variables (e.g., above- and below-canopy PAR, crown dimensions) of the model are more commonly measured in experiments. Thus, we assumed that successful verification of separate sub-routines may be considered as proof of validity of the whole model.

Crown dimensions. For validation of equations for crown size (width and length) we used our own field-collected data on the crown radii of individual trees on mapped sample plots (Shanin et al., 2016; Shashkov et al., 2019) of 1 ha (100 × 100 m). The dataset contains data on the spatial location of each individual tree, its height, DBH, crown radii in four cardinal directions, and crown length. Crown width and crown length for each tree were calculated according to Equations (1–4) and then compared to the measured values. The quality of the model fit was estimated by plotting observed vs. simulated values (Piñeiro et al., 2008). The set of such coordinates was fitted to the linear function $y = s \cdot x$, where slope parameter s and R^2 values were used to evaluate the quality of fit of the modeled vs. the observed values (Figure 3). The validation showed a good fit between measured and simulated crown size. The observed variation could originate from the fact that crown size is affected by more factors than those accounted for in Equations (1–4), e.g., also by wind pattern, relief, wind and pathogen damage, and previous history of the trees' environment (for example, previous competitive pressure from neighboring tree, which does not exist anymore at the moment of observation), but nevertheless, the general trend (slope value) is reproduced very well. However, the model overestimates crown width for large trees. The additional validation was done with the regression-based equivalence test (see Appendix D).

We also validated the model in terms of crown asymmetry using the same dataset. The sum of absolute values of differences between measured and simulated values of crown radii in four cardinal directions was calculated, and then the ratio of this sum to the mean simulated crown radius of given tree was calculated. The mean value of this ratio was 0.44, and that means that for the most of trees the mean deviation of simulated crown radii in given direction did not exceed 22% of measured value. The portion of trees with ratio >1 was 0.038.

PAR below the canopy. To validate the model in terms of the amount of PAR transmitted throughout the canopy, we generated a dataset obtained from corresponding experimental measurements (Galenko, 1983; Johansson, 1989, 1996; Majasalmi et al., 2014; Molchanov, 2000; Navrátil et al., 2007; Olofsson, Eklundh, 2007; Ovhed, Holmgren, 1995; Ozolinčius et al., 1996; Renaud et al., 2011; Walter, Himmler, 1996). We collected only the data where the PAR transmittance was measured over the entire (or almost) vegetation period. The second condition was the presence of data on stand density (or basal area), composition, mean height and DBH of trees, and location. Along with data on direct measurements of PAR interception, we used own experimental estimations (Frolova et al., 2018) of gap light index (GLI) (Canham, 1988), specifying the percentage of incident PAR transmitted through the canopy, based on the analysis of hemispherical photographs. After grouping all records in dataset on the basis of stand age and species composition, the total PAR transmission during the vegetation period was calculated, taking the stand parameters

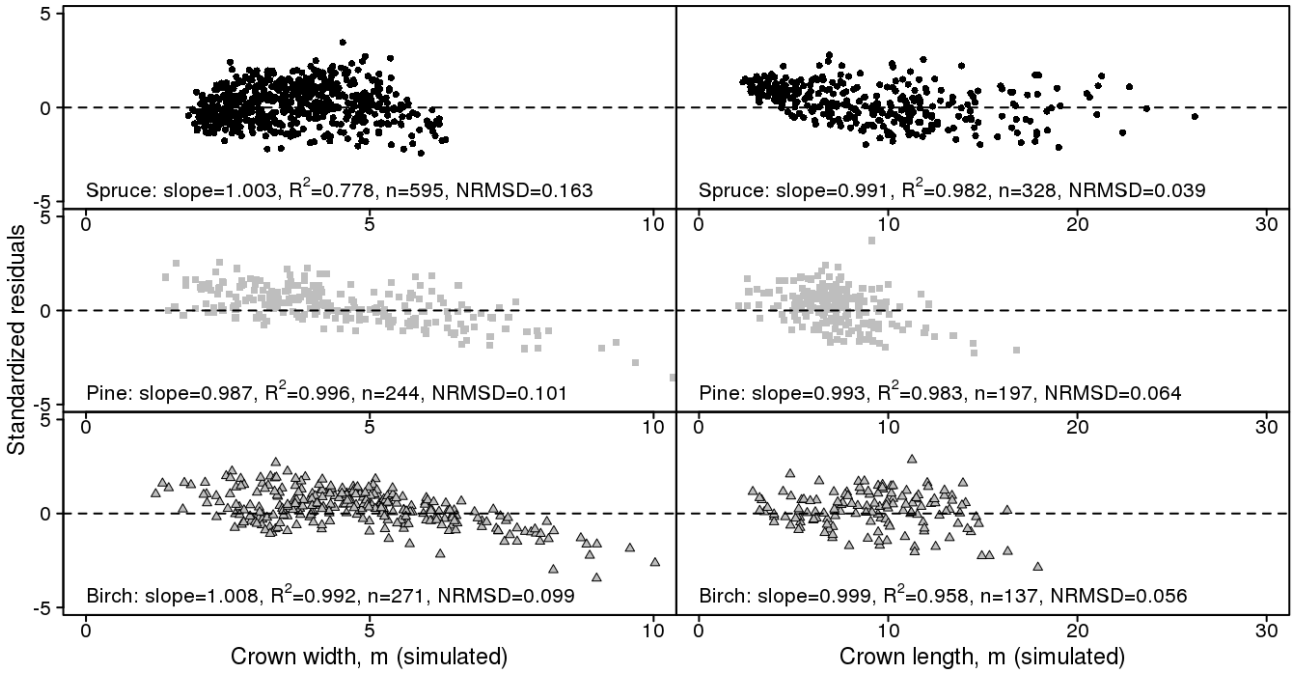

Figure 3: Comparison of predicted vs. observed values of crown dimensions for individual trees (standardized residuals are plotted). Slope value s, goodness-of-fit R^2, number of observations (n), and normalized root mean squared deviation (NRMSD) are also shown.

equal to those presented in the datasets. The mean simulated values of PAR transmittance and their variation for stands of different age groups and composition were then compared to the measured ones (Figure 4). This step required additional calibration of the model: the extinction coefficient (ρ) for pine was increased, since the original model underestimated the absorption of PAR by the pine canopy. Other variations can be explained by the limited number of incoming light directions used in the model. The model was also validated in relation to the radiation above the canopy (Appendix E).

Net primary production. One of possible options can be also the use the combination of several models, where the models of competition provide the amounts of resources (PAR and amount of soil nutrients) captured by each tree as input parameters for the model calculating biomass production, and the calculated increment of each tree (either in terms of net primary production or stem diameter increment) is compared to the corresponding experimental data. First attempts of such verification have been performed previously applying to other model. More details on the integration of models and techniques of simulations can be found in (Shanin et al., 2019). In our case, the latitude was set at 58.6º N, with the vegetation period starting at day 105 (mid-April) and ending at day 288 (mid-October). A set of 100 Monte Carlo runs, with random mixing

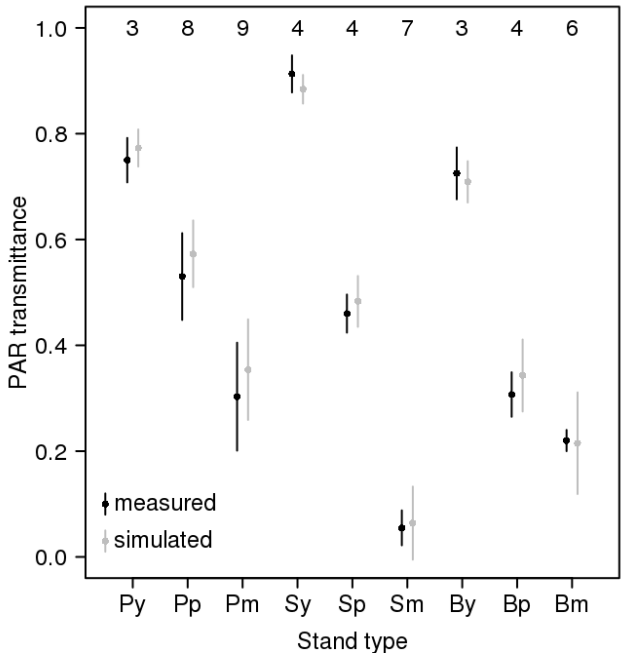

Figure 4: Comparison between measured and simulated values of PAR transmittance throughout the canopies of different compositions. Mean values and standard deviations are shown. Numbers on the upper side denote number of observations.

of positions of trees and a 20% variation of their size, was executed. However, this should be considered as a verification of the combination of models, not only of the model of aboveground competition, therefore the observed deviations from the measured values (for example, simulated NPP was 5–10% higher for young stands in comparison to the measured one, and similar value underestimation of modeled NPP was observed for pole and mature stands (Table 1)) can be related to the uncertainty in parameter estimation of any of the three involved models.

Table 1: Comparison of simulated net primary production (NPP, in terms of carbon) and experimental data (Mencuccini, Grace, 1996; Oleksyn et al., 2000; Xiao et al., 2003; Uri et al., 2007; Shvidenko et al., 2008; Kukumägi et al., 2014; Varik et al., 2015; Usoltsev, 2016b). In experimental data, the stands with age ranging between 1 and 20 years were classified as young, stands with age 21–50 were pole, and stands older than 50 yeas were considered as mature. In simulations the age for young, pole and mature stands was set at 5 (15 for spruce), 30, and 70 years, respectively.

Stand composition and age class	NPP (±SD), $t \cdot ha^{-1} yr^{-1}$	
	simulated	measured
pine, young	2.88 ± 0.24	2.57 ± 0.19
pine, pole	4.27 ± 0.30	4.41 ± 0.39
pine, mature	5.08 ± 0.32	5.36 ± 0.75
spruce, young	2.91 ± 0.29	2.68 ± 0.28
spruce, pole	4.14 ± 0.31	4.16 ± 0.40
spruce, mature	4.26 ± 0.28	4.42 ± 0.59
birch, young	4.61 ± 0.41	4.39 ± 1.21
birch, pole	5.47 ± 0.28	6.11 ± 0.55
birch, mature	5.14 ± 0.45	5.74 ± 0.42

3.2 Sensitivity Analysis

Sensitivity analysis was carried out, and to that end, all parameters of the model were divided into several groups: (i) species-specific parameters describing crown size; (ii) species-specific parameters describing spatial distribution of biomass inside the crown; (iii) species-specific parameters describing overlapping of crowns; (iv) species-specific parameters describing absorption and interception of PAR. Additionally, the influence of basic characteristics of stand (mean height and stem diameter at breast height, stand density) was estimated.

To estimate the sensitivity, a statistical modelling in Monte Carlo mode was used. A uniform variation of each parameter with 100 repetitions within the range of ±25% from the default value (i.e., the value estimated from experimental data - presented in Appendix C) was generated. Each value in obtained range was then combined with set containing other parameters fixed at their default values. Thus, the $100 \cdot n$ sets of parameters were obtained, where n is the total number of parameters. With each set of parameters, the model was executed for single time step (1 year). An uneven-aged spruce stand (see Table 2 below) was used as initial one. The relative absorption of PAR (in GJ per kg of foliage biomass, sum for the whole vegetation season) was chosen as control variable. To estimate the effect of each model parameter, we used the coefficient of variation (standard deviation divided by mean) of the control variable. Since such one-at-a-time approach is often criticized (Saltelli, Annoni, 2010) for its inability to take into account the complexity brought by possible non-linear interactions of parameters, an additional sensitivity analysis has been performed as proposed in (Saltelli, Annoni, 2010). This approach consists in linear regression analysis of standardized values of output variable O with respect to the set of standardized values of input factors $I_1 \ldots I_n$.

Table 2: Initial parameters (± standard deviation) of stands used for simulations. Due to differences in the growth rates of saplings of different species, the age of 5 years was assumed for pine and birch stands, while for spruce stands, the age of 15 years was assumed. However, tree age is not the predictor in any equation of the aboveground competition model and is only used in the productivity model (Shanin et al., 2019). Taking the same size of trees of different species in each age group was assumed to be more substantial for comparison purposes rather than taking the same age of trees. To maintain the comparability, other stand parameters were assumed to be equal among different trees species of the same age group.

Stand type	Age (years)	Density (ha^{-1})	Height (m)	DBH (cm)
young	5, 15	7000	1.70±0.35	1.20±0.45
pole	30	1600	5.00±1.25	7.00±1.25
mature	70	448	22.00±3.30	35.00±3.75
2-layered (canopy)	70	224	22.00±3.30	35.00±3.75
2-layered (undergrowth)	30	800	5.00±1.25	5.00±1.25
uneven-aged	20–230	768	1.90–25.20	4.10–38.90

The standardized regression coefficients $c_0 \ldots c_n$ (subscript $_0$ refers to an intercept) can be considered as the measure of sensitivity, while the value of R^2 shows the non-linearity of the model (the lower the R^2 the higher the non-linearity). Two points (±25% from the default value) were used for each parameter, and then a dataset containing all possible combinations of the parameters were compiled, with the execution of models for one time step for each record in the dataset. Both methods of the analysis showed that the output of model is the most sensitive to parameters affecting crown size. Notably, that in all groups the same parameters were revealed as the most influential ones. Along with the relatively high value of R^2 (0.856) in linear regression, this proves that the effect of parameters on outputs is generally linear. More detailed results of the sensitivity analysis are presented in Appendix F.

3.3 Simulation of Crown Development and PAR Absorption in Stands of Different Composition

To estimate the performance of the model in the simulation of aboveground competition, a set of simulation scenarios was used. All simulations were carried out on virtual plot of 50 × 50 m, divided into square cells of 0.5 × 0.5 m. To eliminate the edge effect, the «wrapping around the torus» was used (Haefner et al., 1991). The set of scenarios allows the simulation of stands of different development stages and spatial structures (Table 2). Simulated stands consisted of spruce, pine, and birch in different combinations (both pure stands and two-species mixtures with species proportions of 50:50%). Three types of spatial structure were simulated: regular (allocation of trees on a regular grid), random, and allocation of trees in several dense clusters, according to the Neyman-Scott algorithm (Illian et al., 2008)). The allocation and sizes of trees for the uneven-aged stand was based on experimental data (Shanin et al., 2016; Shashkov et al., 2019).

The simulation results were analyzed on the basis of several output variables at individual- and stand-level: (i) relative crown height; (ii) relative crown width; (iii) spatial distribution of aboveground biomass; (iv) PAR absorption; (v) spatial distribution of PAR below the canopy.

The simulations showed that relative crown length (ratio of crown length to total tree height) is dependent on stand age, being lower in mature stands (0.4–0.5 for birch and pine, 0.7–0.8 for spruce) than in young and pole stands (0.5 for birch, 0.8–0.9 for pine, 0.9–0.95 for spruce). The crown length of birch decreased by about 5% in the mixture with spruce, and mixture with pine resulted in a 5% increase in crown length in comparison to the pure birch stand. Pine increased crown length by 10% in mixture with spruce, and no remarkable changes were observed when mixed with birch. The crown length of spruce increased by 5% in mixtures both with pine and birch in comparison to pure spruce stands. The relative crown width is characterized by a similar pattern, but an increased variation of this parameter was observed in mixed stands.

As expected, the simulated density of foliage biomass (in $kg \cdot m^{-2}$) also increased with stand age due to increased canopy height, providing more space for aboveground tree organs. The mean value was 0.2–0.3 $kg \cdot m^{-2}$ in young stands and 0.4–0.8 $kg \cdot m^{-2}$ in pole and mature stands. However, in some cells for pine and birch stands, the values reached 1 $kg \cdot m^{-2}$, while spruce stands were characterized by the highest values (up to 3 $kg \cdot m^{-2}$ in some cells) due to the more compact crowns of spruce in comparison to pine and, in particular, birch. Spatial stand structure (within the simulated variation of densities) had no significant effect on biomass density.

The increased efficiency of PAR interception in mixed stands, in comparison to monocultures, was also observed. For example, in a young pure pine stand with random tree allocation, the value of specific PAR absorption was 4.237 GJ per kg of foliage during the vegetation period. In the young pure birch stand, this value was 4.585. The expected value of specific absorption in a mixed stand (50% pine and 50% birch) can be calculated as the arithmetic mean of these two values (4.411 GJ per kg of foliage during the vegetation period) while the simulated value was 4.505 (2.1% higher than expected).

We also calculated the specific tree-wise absorption of PAR (sum throughout the entire vegetation season) in GJ per 1 kg of foliage biomass. The highest values of specific absorption were shown for birch, while in coniferous species, the specific absorption was lower (especially in spruce), which might be related to the differences in leaf area density (e.g., relation between leaf biomass and leaf area). No significant differences in specific absorption between stands of different spatial structure were found, but nevertheless, the same pattern was noted in all cases where the specific absorption at a clustered tree allocation was slightly lower and slightly higher at a regular allocation in comparison to random allocation. Similar trends were observed in pole stands, but with higher variations inside each case study as a result of the variation in tree size, which increases with stand age.

The relative increase in absorption efficiency in mixed stands, in comparison to pure ones, was 7.6% for a mixture of equal portions of pine and birch and 8.1% for a mixture of equal portions of spruce and birch. Notably, the relative increase in PAR interception efficiency was higher in the stand comprised of species with more different strategies in relation to light use. Mature

stands showed similar patterns, albeit with lower values of specific PAR absorption. Both mixed two-layered and uneven-aged spruce stands had higher variations in this value due to the presences of differently sized trees (Figure 5).

Analysis of the PAR distribution below the canopy showed that strongly shaded cells (PAR below the canopy is less than 10% of above-canopy PAR) are absent in young stands. The portion of cells with high portions of PAR transmitted through the canopy was higher in coniferous stands, which can be explained by the more compact crowns of these species. However, it should be noted that the same number and size of trees for stands of the same age group was set, irrespective of the species composition (to simplify the comparison), while actually, the "normal" density of stands of the same age is dependent on tree species composition. Therefore, young conifer stands provide some portions of "gaps" in the canopy (corresponding to cells with ratios of below- to above-PAR close to 1). We also showed that at a regular tree distribution, the range of values of PAR below the canopy was narrower than at other types of spatial structure. In particular, young mixed stands comprised of equal portions of pine and birch showed a more homogeneous filling of space by the tree crowns, thus resulting in the absence of breaks in the distribution; in contrast to birch stands, strongly shaded cells were absent (Figure 6).

As expected, in pole stands, the portion of strongly shaded cells increased, and the distribution of PAR below the canopy became more homogeneous. However, the differences between stands of both different species composition and spatial structure remained remarkable, being similar, but nevertheless lower than in young stands. Mature stands, as expected, showed the highest portion of strongly shaded cells. In contrast to young and pole stands, in mature spruce stands, strong shading was observed, with a relatively high portion of cells with a ratio of below- to above-PAR close to 0, while in pine stands, the portion of such cells was the lowest, probably because of the higher crown length and needle biomass density per unit of crown volume in spruce stands. Mixed stands were characterized by a more homogeneous distribution of PAR below the canopy, with a higher portion of strongly shaded cells in the spruce-birch mixture in comparison to the pine-spruce mixture,

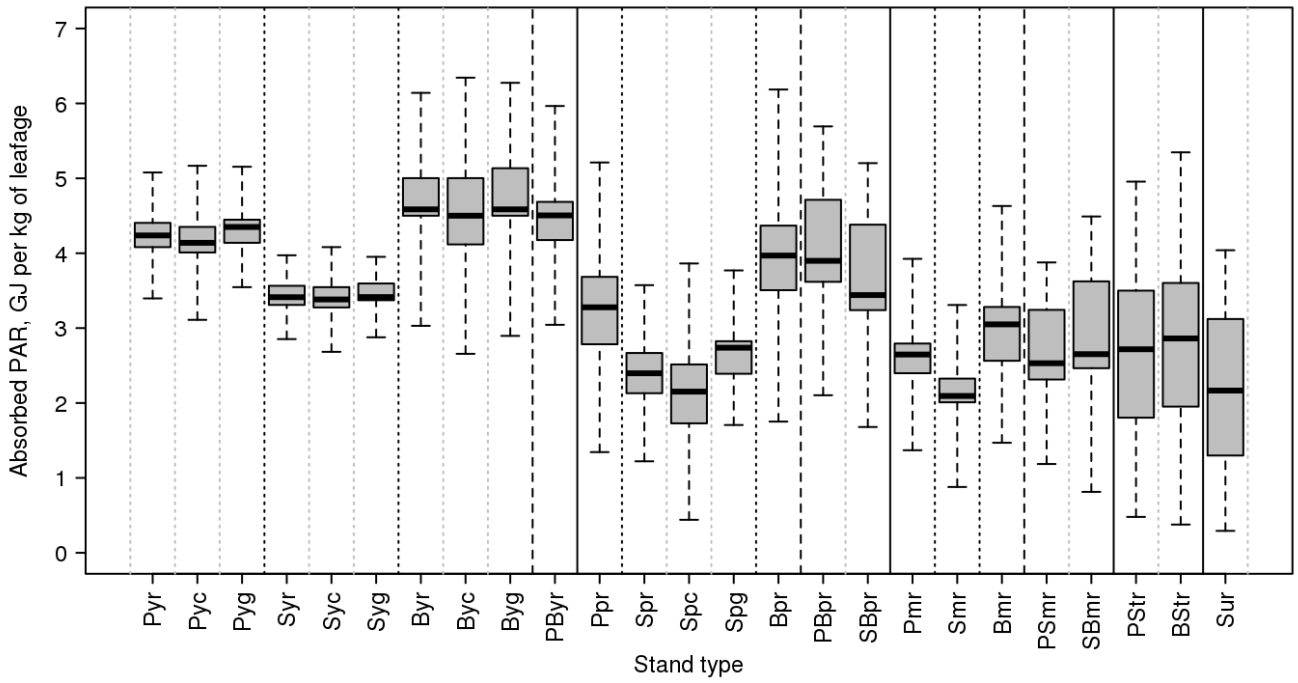

Figure 5: Simulated specific PAR absorption during the vegetation period (per 1 kg of foliage biomass) in stands of different species composition, age, and spatial structure. Here and below, the following scenario codes are used: uppercase letters denote tree species ("P" - pine, "S" - spruce, "B" - birch), lowercase letter denote age group ("y" - young, "p" - pole, "m" - mature, "t" - two layered (first species in the canopy, and the second one in the undergrowth), "u" - uneven-aged) and spatial structure ("r" - random placement of trees, "c" - clustered placement, "g" - regular placement on square grid) of stands. Median values (thick horizontal line), 1st and 3rd quartiles (boxes), and triple standard deviation (whiskers) are shown.

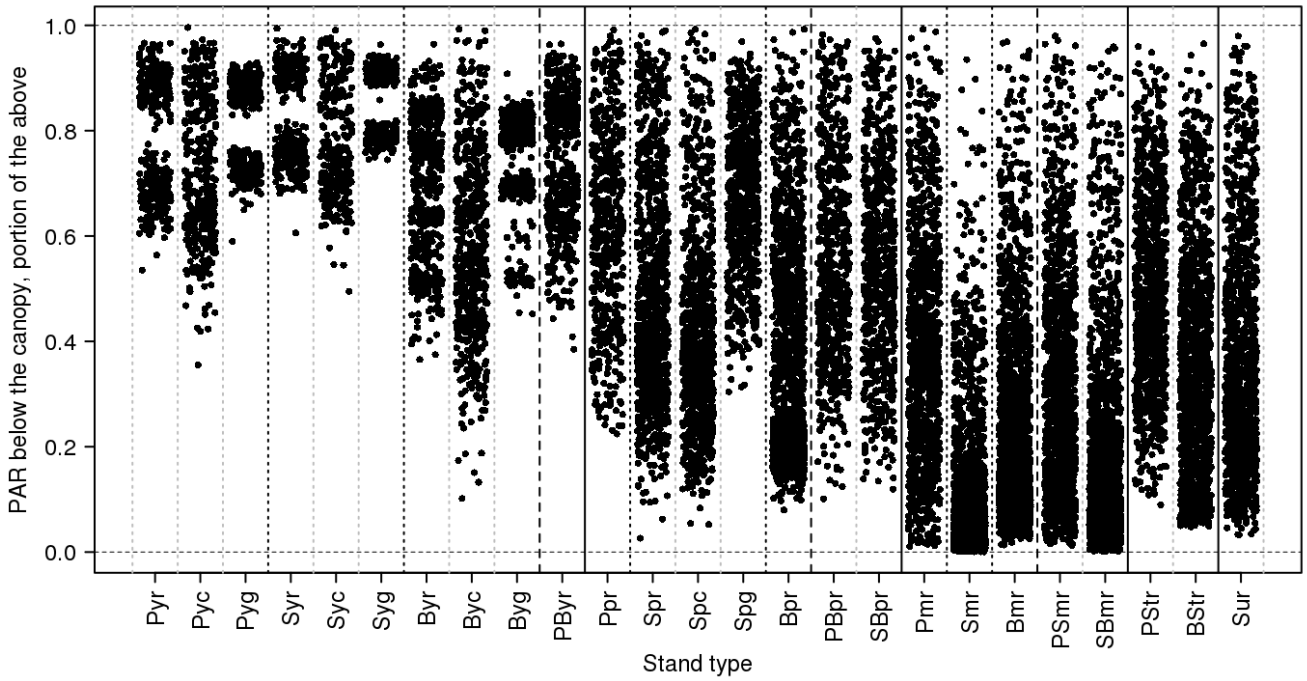

Figure 6: Simulated spatial distribution of PAR below the canopy, expressed as portion of PAR above the canopy (for the area used in the simulation, the total PAR above the canopy during the vegetation season was 1.376 $GJ \cdot m^{-2}$). Each point corresponds to the value of PAR below the canopy in the individual cell of the simulation plot; the cells containing the stem base were excluded. Scenario codes are the same as in Figure 5.

due to differences in the light permeability of crowns. Two-layered stands (with the canopy being comprised of pine or birch and spruce in the undergrowth) and uneven-aged spruce stands, with the most complex spatial structure (combining high-density groups of mature trees and gaps with smaller trees) had no completely shaded cells.

Crown asymmetry was estimated based on the coefficient C_a:

$$C_a = \frac{\begin{array}{c}|R_{mean} - R_N| + |R_{mean} - R_E| + \\ |R_{mean} - R_S| + |R_{mean} - R_W|\end{array}}{4 \cdot R_{mean}}, \qquad (10)$$

where R_N, R_E, R_S, and R_W are crown radii in northern, eastern, southern, and western directions, respectively, and R_{mean} is the mean crown radius, calculated as follows:

$$R_{mean} = \frac{R_N + R_E + R_S + R_W}{4}. \qquad (11)$$

The calculated crown asymmetry increased from spruce (median value of 0.142) to pine (0.247) and birch (0.363) and was generally 7–12% higher in mixed stands in comparison to monocultures; this finding is in agreement with our previously published results (Shanin et al., 2016). For birch and pine, the asymmetry was about 30% lower in young stands in comparison to mature ones, while for spruce, we found no differences among stands of different ages. To check the model performance related to the simulation of crown asymmetry, we compared the efficiency of PAR interception obtained with the "full model" and the PAR interception obtained from the model where the asymmetry was disabled (all crowns were represented as axisymmetric bodies without distortion of their horizontal expansion in different directions due to competition). The comparison showed that taking into account the asymmetry increases the PAR absorption by 12–23%, depending on the stand structure.

4 DISCUSSION

The simulated crown length indicates that competition remains an important factor throughout stand development, while other factors (spatial structure and species composition) have no considerable influence on relative crown height. The decrease in relative crown height is related to the dieback of branches in the lower parts of the crowns, where the metabolic cost of maintaining living biomass is higher than the gain obtained via photosynthesis. The simulations also showed that in mixed stands formed by species with different strategies in relation to above-ground competition, both or one of

the species receives an advantage, in comparison to pure stands, due to more efficient canopy space filling (Pretzsch, 2014).

Some differences in PAR absorption at different spatial allocation of trees can be observed because in young stands, where the canopy is not yet closed, the regular allocation of trees is the most optimal one for stand-level interception of PAR because it provides the space for crown expansion for all trees, while at random and, especially, clustered allocation of trees, some crowns may overlap, thus increasing the strength of competition for light and, as a result, reducing the total amount of intercepted PAR. However, during stand development, crowns are close-up, and regular allocation becomes less optimal since all trees have the same number of neighbors. In contrast, in stands with irregular spatial structure, some trees may have an advantage due to lower competitive pressure. At the stand level, this may result in a higher interception of PAR. This difference of specific PAR absorption in mixed stands, in comparison to monocultures, seems to be small but it shows how the model represents the effect of "niche segregation" among tree species (Sterba et al., 2002; Cavard et al., 2011) due to species-specific differences in crown shape and biomass allocation inside the crown, which results in a more efficient occupation of space and interception of PAR. The specific PAR absorption generally decreased with stand age, which could be related to the increased crown size, which, in turn, increases the length of the beam path through the canopy and, consequently, the number of cells which receive relatively small amounts of incoming solar radiation.

The breaks in the distribution of PAR values below the canopy, observed in young stands at random, and the regular spatial structure can be considered as "artifacts" originating from the shortcomings of the calculation procedure, where crown volume and biomass distribution are represented by discrete cells. For small trees in young stands, each individual crown was represented by the relatively small number of cells, and discrete calculation of PAR transmittance resulted in breaks in the distribution of calculated values. Notably, at a clustered initial allocation of trees, such breaks were not observed, most likely because of the more complex structure as a result of the combination of "gaps" and zones with high crown overlapping.

5 CONCLUSIONS

The suggested approach can be considered as a hybrid between two most commonly used ones: (i) detailed models with explicit representation of crown architecture and scattering of incoming PAR with highly-accurate calculation of ray-tracing, but requiring a large number of input parameters; and (ii) simplified models which represent the forest canopy as several horizontal layers and the tree crowns as a volume or plane geometric figures with a homogeneous inner structure. The used approach enables the simulation of light absorption by the canopy with a high spatial resolution using relatively few parameters.

The important features of the suggested model are: (i) taking into account the spatial distribution inside the crown of both photosynthesizing and non-photosynthesizing organs; (ii) an adaptive concept of algorithms when the biomass inside the crown is distributed in a way that decreases the strength of competition between individual trees in the stand; (iii) relative simplicity of the algorithm and a small number of parameters (compared to the 3-dimensional models). Such features will allow us to include the model of aboveground competition into the system of models EFIMOD, which simulates the population dynamics and biological turnover of basic nutrients in mixed uneven-aged boreal forest stands.

The proposed model uses species-specific parameters and pays special attention to the simulation of asymmetry in crown shape and biomass distribution as a result of competition between individuals, thus enabling the simulation of aboveground competition in mixed uneven-aged stands.

6 ACKNOWLEDGMENTS

The study was supported by the Russian Science Foundation, project #18-14-00362 (analysis of data, development, calibration, and verification of the model) and the Russian Foundation for Basic Research, project #18-04-00527 (collecting of experimental data for model calibration and verification). The work of Natalya Ivanova was partly done in frames of Basic Scientific Research theme of the Institute of Mathematical Problems of Biology RAS - the Branch of Keldysh Institute of Applied Mathematics of Russian Academy of Sciences. We are also very grateful to the three anonymous reviewers for the careful reading and constructive comments which helped us to improve the quality of the paper, and to the Editor for handling our manuscript.

References

Anonymous. 1987–2001. Scientific and applied reference book on climate of USSR [Nauchno-prikladnoy spravochnik po klimatu SSSR]. Issues 1–34. Leningrad (Saint Petersburg), Gidrometeoizdat. (In Russian).

Aubin, I., Beaudet, M., & Messier, C. 2000. Light extinction coefficients specific to the understory vegetation

of the southern boreal forest, Quebec. Can. J. For. Res. 30: 168–177. doi:10.1139/x99–185

Bobkova, K.S., Urnyshev, A.P., & Urnyshev, V.A. 2000. Vertical distribution of phytomass in spruce forests of European north-east [Vertikal'noe raspredelenie fitomassy v elovykh lesakh evropeiskogo severo-vostoka]. Lesovedenie 3: 49–54. (In Russian).

Bossel, H. 1996. TREEDYN3 forest simulation model. Ecol. Model. 90. 187–227. doi:10.1016/0304–3800(95)00139-5

Brisson, J. 2001. Neighborhood competition and crown asymmetry in *Acer saccharum*. Can. J. For. Res. 31: 2151–2159. doi:10.1139/x01-161

Canham, C.D. 1988. An index for understory light levels in and around canopy gaps. Ecology 69: 1634–1638. doi:10.2307/1941664

Cavard, X., Bergeron, Y., Chen, H.Y.H., Paré, D., Laganiére, J., & Brassard, B. 2011. Competition and facilitation between tree species change with stand development. Oikos 120: 1683–1695. doi:10.1111/j.1600-0706.2011.19294.x

Cescatti, A. 1997a. Modelling the radiative transfer in discontinuous canopies of asymmetric crowns. I. Model structure and algorithms. Ecol. Model. 101(2–3): 263–274. doi:10.1016/S0304-3800(97)00050-1

Cescatti, A. 1997b. Modelling the radiative transfer in discontinuous canopies of asymmetric crowns. II. Model testing and application in a Norway spruce stand. Ecol. Model. 101(2–3): 275–284. doi:10.1016/S0304-3800(97)00055-0

Cieszewski, C., Strub, M., Antony, F., Bettinger, P., Dahlen, J., & Lowe, R. 2013. Wood quality assessment of tree trunk from the tree branch sample and auxiliary data based on NIR Spectroscopy and SilviScan. Mathematical and Computational Forestry & Natural-Resource Sciences (MCFNS), 5(1), 86–111 (26). Retrieved from http://mcfns.net-/index.php/Journal/article/view/155

Collalti, A., Perugini, L., Santini, M., Chiti, T., Nolèc, A., Matteucci, G., & Valentini, R. 2014. A process-based model to simulate growth in forests with complex structure: Evaluation and use of 3D-CMCC Forest Ecosystem Modeling a deciduous forest in Central Italy. Ecol. Model. 272: 362–378. doi:10.1016/j.ecolmodel.2013.09.016

Daniels, R.F., Burkhart, H.E., & Clason, T.R. 1986. A comparison of competition measures for predicting growth of loblolly pine trees. Can. J. For. Res. 16: 1230–1237. doi:10.1139/x86-218

Danilov, D.A. & Ischuk, T.A. 2013. Competitive relationships in the pine-spruce stands undergone improvement thinning and complex forest care [Otsenka konkurentnykh vzaimootnosheniy sosny i eli v smeshannykh drevostoyakh chernichnogo tipa lesa, proidennykh rubkami ukhoda i kompleksnym ukhodom za lesom]. Sistemy. Metody. Tekhnologii 1(17): 176–181. (In Russian with English summary).

Duursma, R.A. & Mäkelä, A. 2007. Summary models for light interception and light-use efficiency of non-homogeneous canopies. Tree Physiol. 27: 859–870. doi:10.1093/treephys/27.6.859

Evstigneev, O.I. 2018. Ontogenetic scales of relation of trees to light (on the example of eastern European forests). Russ. J. Ecosyst. Ecol. 3(3). doi:10.21685/2500-0578-2018-3-3

Frolova, G., Frolov, P., Ivanova, N., & Shanin, V. 2018. Analysis of competitive interactions between undergrowth and ground layer vegetation in pine forests of the European part of Russia. In M. Zhiyanski, M. Glushkova, & M. Georgieva (eds.) International scientific conference "90 years Forest research institute - for the society and nature", 24–26 October 2018, Sofia, Bulgaria. Book of abstracts. P. 56.

Galenko, E.P. 1983. Phytoclimate and energetic factors of productivity of coniferous forest of European North [Fitoklimat I energeticheskie factory produktivnosti khvoynogo lesa Evropeyskogo severa]. Leninrad, Nauka. (In Russian).

Garcia, O. (2014). A generic approach to spatial individual-based modelling and simulation of plant communities. Mathematical and Computational Forestry & Natural-Resource Sciences (MCFNS), 6(1), 36–47 (12). Retrieved from http://mcfns.net/-index.php/Journal/article/view/6_36

Gower, S.T., McMurtrie, R.E., & Murty, D. 1996. Aboveground net primary production decline with stand age: potential causes. Trends Ecol. Evol. 11(9): 378–382. doi:10.1016/0169-5347(96)10042-2

Green, D.G. & Sadedin, S. 2005. Interactions matter - complexity in landscapes and ecosystems. Ecol. Complex. 2: 117–130. doi:10.1016/j.ecocom.2004.11.006

Gspaltl, M., Bauerle, W., Binkley, D., & Sterba, H. 2013. Leaf area and light use efficiency patterns of Norway spruce under different thinning regimes and age classes. For. Ecol. Manage. 288: 49–59. doi:10.1016/j.foreco.2011.11.044

Gulbe, Ya.I., Ermolova, L.S., Rozhdestvenskiy, S.G., Utkin, A.I., & Tselniker, Yu.L. 1983. Vertical distribution of leaf surface and light regime in hardwood young stands of southern taiga [Vertikal'noe raspredelenie poverkhnosti list'ev i svetovoy rezhim v listvennykh molodnyakakh yuzhnoi taygi]. Lesovedenie 2: 21–29. (In Russian with English summary).

Haywood, A. 2002. Growth of advanced European beech trees in the transformation phase in the southern Black Forest. [Dissertation] University of Freiburg. 152 p.

Haefner, J.W., Poole, G.C., Dunn, P.V., & Decker, R.T. 1991. Edge effects in computer models of spatial competition. Ecol. Model. 56: 221–244. doi:10.1016/0304-3800(91)90201-B

Iles, K. (2009). "Nearest-tree" estimations - A discussion of their geometry. Mathematical and Computational Forestry & Natural-Resource Sciences (MCFNS), 1(2), Pages: 47–51 (5). Retrieved from http://mcfns.net/index.php/Journal/article/view/MCFNS.1-47

Illian, J., Penttinen, A., Stoyan, H., & Stoyan, D. 2008. Statistical analysis and modelling of spatial point patterns. John Wiley & Sons. 560 p. ISBN: 978-0-470-01491-2.

Johansson, T. 1989. Irradiance within canopies of young trees of European aspen (*Populus tremula*) and European birch (*Betula pubescens*) in stands of different spacings. For. Ecol. Manage. 28: 217–236. doi:10.1016/0378-1127(89)90005-4

Johansson, T. 1996. Estimation of canopy density and irradiance in 20- and 40-year-old birch stands (*Betula pubescens* Ehrh. and *Betula pendula* Roth). Trees 10: 223–230. doi:10.1007/BF02185673

Kędra, K. & Gazda, A. 2016. New angular competition index and crown projection model. Abstracts of 2016 IEEE International Conference on Functional-Structural Plant Growth Modeling, Simulation, Visualization and Applications, 7–11 Nov, Qingdao, China. P. 13.

Kolobov, A.N. & Frisman, E.Ya. 2016. Individual-based model of spatio-temporal dynamics of mixed forest stands. Ecol. Complex. 27: 29–39. doi:10.1016/j.ecocom.2015.10.002

Komarov, A., Chertov, O., Zudin, S., Nadporozhskaya, M., Mikhailov, A., Bykhovets, S., Zudina, E., & Zoubkova, E. 2003. EFIMOD 2 - A model of growth and elements cycling in boreal forest ecosystems. Ecol. Model. 170(2–3): 373–392. doi:10.1016/S0304-3800(03)00240-0

Kukumägi, M., Ostonen, I., Kupper, P., Truu, M., Tulva, I., Varik, M., Aosaar, J., Sõber, J., & Lõhmus, K. 2014. The effects of elevated atmospheric humidity on soil respiration components in a young silver birch forest. Agric. For. Meteorol. 194: 167–174. doi:10.1016/j.agrformet.2014.04.003

Lebedev, A.N., Borushko, I.S., & Egorova, A.Yu. (Eds). 1979. Reference book on climate of Western Europe [Klimaticheskiy spravochnik Zapadnoi Evropy]. Leningrad, Gidrometeoizdat. (In Russian). 678 p.

Lebedev, S.V. & Chumachenko, S.I. 2002. Dynamic model of uneven-aged mixed-species forest community: modelling the light regime under the canopy [Dinamicheskaya model' raznovozrastnogo mnogovidovogo lesnogo tsenoza: modelirovanie svetovogo rezhima pod pologom]. In Ecology, monitoring and rational use of natural resources: transactions [Ekologiya, monitoring i ratsional'noe prirodopol'zovanie. Nauchnye trudy]. Issue 318. Moscow, Moscow state forest university. P. 111–118. (In Russian).

Lebedev, S.V. & Chumachenko, S.I. 2011. Individual-based dynamic model of mixed uneven-aged stand (PIXTA) [Poderevnaya model' dinamiki mnogovidovogo raznovozrastnogo nasazhdeniya (PIXTA)]. Vestnik Moskovskogo gosudarstvennogo universiteta lesa - Lesnoy vestnik 7(83): 73–80. (In Russian).

Lintunen, A., Kaitaniemi, P., Perttunen, J., & Sievänen, R. 2013. Analysing species-specific light transmission and related crown characteristics of *Pinus sylvestris* and *Betula pendula* using a shoot-level 3D model. Can. J. For. Res. 43: 929–938. doi:10.1139/cjfr-2013-0178

Majasalmi, T., Rautiainen, M., & Stenberg, P. 2014. Modeled and measured fPAR in a boreal forest: Validation and application of a new model. Agric. For. Meteorol. 189–190: 118–124. doi:10.1016/j.agrformet.2014.01.015

Mäkelä, A. & Vanninen, P. 2001. Vertical structure of Scots pine crowns in different age and size classes. Trees 15: 385–392. doi:10.1007/s004680100118

McCree, K.J. 1981. Photosynthetically active radiation. In Encyclopedia of Plant Physiology, vol. 12A. Springer-Verlag, Berlin, P. 41–55.

Mencuccini, M. & Grace, J. 1996. Hydraulic conductance, light interception and needle nutrient concentration in Scots pine stands and their relations with net primary productivity. Tree Physiol. 16: 459–468. doi:10.1093/treephys/16.5.459

Molchanov, A.G. 2000. Photosynthetic utilization efficiency of absorbed photosynthetically active radiation by Scots pine and birch forest stands in the southern Taiga. Tree Physiol. 20: 1137–1148. doi:10.1093/treephys/20.17.1137

Morin, X., Fahse, L., Scherer-Lorenzen, M., & Bugmann, H. 2011. Tree species richness promotes productivity in temperate forests through strong complementarity between species. Ecol. Lett. 14: 1211–1219. doi:10.1111/j.1461-0248.2011.01691.x

Navrátil, M., Špunda, V., Marková, I., & Janous, D. 2007. Spectral composition of photosynthetically active radiation penetrating into a Norway spruce canopy: the opposite dynamics of the blue/red spectral ratio during clear and overcast days. Trees 21: 311–320. doi:10.1007/s00468-007-0124-4

Olchev, A., Radler, K., Sogachev, A., Panferov, O., & Gravenhorst, G. 2009. Application of a three-dimensional model for assessing effects of small clear-cuttings on radiation and soil temperature. Ecol. Model. 220: 3046–3056. doi:10.1016/j.ecolmodel.2009.02.004

Oleksyn, J., Reich, P.B., Rachwal, L., Tjoelker, M.G., & Karolewski, P. 2000. Variation in aboveground net primary production of diverse European *Pinus sylvestris* populations. Trees 14: 415–421. doi:10.1007/PL00009775

Olofsson, P. & Eklundh, L. 2007. Estimation of absorbed PAR across Scandinavia from satellite measurements. Part II: Modeling and evaluating the fractional absorption. Remote Sens. Environ. 110: 240–251. doi:10.1016/j.rse.2007.02.020

Ovhed, M. & Holmgren, B. 1995. Spectral Quality and Absorption of solar radiation in a mountain birch forest, Abisko, Sweden. Arctic Alpine Res. 27(4): 380–388. doi:10.1080/00040851.1995.12003135

Ozolinčius, R., Mikšys, V., & Stakénas, V. 1996. Above-ground phytomass and light regime in Norway spruce stands planted with different initial density. Biomass Bioenerg. 11(2/3): 201–206. doi:10.1016/0961-9534(96)00015-3

Peng, C., Liu, J., Dang, Q., Apps, M.J., & Jiang, H. 2002. TRIPLEX: a generic hybrid model for predicting forest growth and carbon and nitrogen dynamics. Ecol. Model. 153: 109–130. doi:10.1016/S0304-3800(01)00505-1

Perttunen, J. 2009. The LIGNUM functional-structural tree model. [Dissertation] Systems Analysis Laboratory, Helsinki University of Technology. 52 p.

Piñeiro, G., Perelman, S., Guerschman, J.P., & Paruelo, J.M. 2008. How to evaluate models: observed vs. predicted or predicted vs. observed? Ecol. Model. 216: 316–322. doi:10.1016/j.ecolmodel.2008.05.006

Pretzsch, H., Biber, P., & Ďurský, J. 2002. The single tree-based stand simulator SILVA: construction, application and evaluation. For. Ecol. Manage. 162: 3–21. doi:10.1016/S0378-1127(02)00047-6

Pretzsch, H. 2014. Canopy space filling and tree crown morphology in mixed-species stands. For. Ecol. Manage. 327: 251–264. doi:10.1016/j.foreco.2014.04.027

Pretzsch, H. & Schütze, G. 2016. Effect of tree species mixing on the size structure, density, and yield of forest stands. Eur. J. For. Res. 135: 1–22. doi:10.1007/s10342-015-0913-z

Pugachevskiy, A.V. 1992. Coenopopulations of spruce: structure, dynamics, regulating factors [Tsenopopulyatsii eli: struktura, dinamika, faktory regulyatsii]. Minsk, Navuka i tekhnika. (In Russian).

R Core Team. 2014. R: A language and environment for statistical computing. R Foundation for Statistical Computing, Vienna, Austria.

Rautiainen, M. & Stenberg, P. 2005. Simplified tree crown model using standard forest mensuration data for Scots pine. Agric. For. Meteorol. 128: 123–129. doi:10.1016/j.agrformet.2004.09.002

Renaud, V., Innes, J.L., Dobbertin, M., & Rebetez, M. 2011. Comparison between open-site and below-canopy climatic conditions in Switzerland for different types of forests over 10 years (1998–2007). Theor. Appl. Climatol. 105: 119–127. doi:10.1007/s00704-010-0361-0

Renshaw, E. 1985. Computer simulation of Sitka spruce: spatial branching models for canopy growth and root structure. Math. Med. Biol. 2: 183–200. doi:10.1093/imammb/2.3.183

Repola, J. 2006. Models for vertical wood density of Scots pine, Norway spruce and birch stems, and their application to determine average wood density. Silva Fenn. 40(4): 673–685.

Robinson, A.P., Duursma, R.A. & Marshall, J.D. 2005. A regression-based equivalence test for model validation: shifting the burden of proof. Tree Physiol. 25: 903–913. doi:10.1093/treephys/25.7.903

Ross, J. 1981. The radiation regime and architecture of plant stands. Dr W. Junk Publishers, The Hague. 420 p. doi:10.1007/978-94-009-8647-3

Rouvinen, S. & Kuuluvainen, T. 1997. Structure and asymmetry of tree crowns in relation to local competition in a natural mature Scots pine forest. Can. J. For. Res. 27:. 890–902. doi:10.1139/x97-012

Saltelli, A. & Annoni, P. 2010. How to avoid a perfunctory sensitivity analysis. Environ. Model. Softw. 25(12):1508–1517. doi: 10.1016/j.envsoft.2010.04.012

Schröter, M., Härdtle, W., & von Oheimb, G. 2012. Crown plasticity and neighborhood interactions of European beech (*Fagus sylvatica* L.) in an old-growth forest. Eur. J. For. Res. 131: 787–798. doi:10.1007/s10342-011-0552-y

Seidl, R., Rammer, W., Scheller, R.M., & Spies, T.A. 2012. An individual-based process model to simulate landscape-scale forest ecosystem dynamics. Ecol. Model. 231: 87–100. doi:10.1016/j.ecolmodel.2012.02.015

Shanin, V.N., Shashkov, M.P., Ivanova, N.V., & Grabarnik, P.Ya. 2016. The effect of aboveground competition on spatial structure and crown shape of the dominating canopy species of forest stands of European Russia [Vliyanie konkurentsii v pologe lesa na prostranstvennuyu strukturu drevostoev i formu kron dominantov drevesnogo yarusa na primere lesov evropeiskoi chasti Rossii]. Russ. J. Ecosyst. Ecol. 1(4). doi:10.21685/2500-0578-2016-4-5 (In Russian with English summary).

Shanin, V.N., Grabarnik, P.Ya., Bykhovets, S.S., Chertov, O.G., Priputina, I.V., Shashkov, M.P., Ivanova, N.V., Stamenov, M.N., Frolov, P.V., Zubkova, E.V., & Ruchinskaya, E.V. 2019. Parameterization of productivity model for the most common trees species in European part of Russia for simulation of forest ecosystem dynamics [Parametrizatsiya modeli produktsionnogo protsessa dlya dominiruyushchikh vidov derev'ev Evropeyskoy chasti RF v zadachakh modelirovaniya dinamiki lesnykh ekosistem]. Math. Biol. Bioinformatics 14(1). doi: 10.17537/2019.14.54 (In Russian with English summary).

Shashkov, M., Ivanova, N., Shanin, V., & Grabarnik, P. 2019. Ground surveys versus UAV photography: the comparison of two tree crown mapping techniques. In I. Bychkov & V. Voronin (eds.). Information Technologies in the Research of Biodiversity. Springer Proceedings in Earth and Environmental Sciences. Springer, Cham. P. 48–56. doi: 10.1007/978-3-030-11720-7_8

Shvidenko, A.Z., Schepaschenko, D.G., Nilsson, S., & Buluy, Yu.I. 2008. Tables and models of growth and productivity of forests of major forest forming species of Northern Eurasia (standard and reference materials). Second edition, supplemented. Moscow, Federal Agency Of Forest Management, International Institute For Applied Systems Analysis. 886 p.

Sterba, H., Blab, A., & Katzensteiner, K. 2002. Adapting as individual tree growth model for Norway spruce (*Picea abies* L. Karst.) in pure and mixed species stands. For. Ecol. Manage. 159: 101–110. doi:10.1016/S0378-1127(01)00713-7

Stoll, P. & Schmid, B. 1998. Plant foraging and dynamic competition between branches of *Pinus sylvestris* in contrasting light environments. J. Ecol. 86: 934–945. doi:10.1046/j.1365-2745.1998.00313.x

Tahvanainen, T. & Forss, E. 2008. Individual tree models for the crown biomass distribution of Scots pine, Norway spruce and birch in Finland. For. Ecol. Manage. 255: 455–467. doi:10.1016/j.foreco.2007.09.035

Thorpe, H.C., Astrup, R., Trowbridge, A., & Coates, K.D. 2010. Competition and tree crowns: a neighborhood analysis of three boreal tree species. For. Ecol. Manage. 259: 1586–1596. doi:10.1016/j.foreco.2010.01.035

Tran, Q.T., Tainar, D., & Safar, M. 2009. Reverse k nearest neighbor and reverse farthest neighbor search on spatial networks. In A. Hameurlain, J. Küng, & R. Wagner (eds.). Transactions on large-scale data- and knowledge-centered systems. 374 p. doi:10.1007/978-3-642-03722-1.

Tselniker, Yu.L., Malkina, I.S., Gurtsev, A.I., & Nikolayev, D.K. 1999. Quantitative estimation of light regime based on morphostructural indicators of crowns of spruce saplings [Kolichestvennaya otsenka svetovogo rezhima po morfostrukturnym pokazatelyam kron podrosta eli]. Lesovedenie 4: 64–69. (In Russian).

Usoltsev, V.A. 2013a. Structure of tree biomass-height profiles: studying a system of regularities [Vertikal'no-fraktsionnaya struktura fitomassy derev'ev. Issledovanie zakonomernostey]. Ekaterinburg, Ural State Forest Engineering University. 602 p. (In Russian with English summary).

Usoltsev, V.A. 2013b. Production and competitive relations of trees: studying a system of regularities [Produktsionnye pokazateli i konkurentnye otnosheniya derev'ev. Issledovanie zavisimostei]. Ekaterinburg, Ural State Forest Engineering University. 553 p. (In Russian with English summary).

Usoltsev, V.A. 2016a. Single-tree biomass of forest-forming species in Eurasia: database, climate-related geography, weight tables [Fitomassa model'nykh derev'ev lesoobrazuyushchikh porod Evrazii: baza dannykh, klimaticheski obuslovlennaya geografiya, taksatsionnye normativy]. Ekaterinburg, Ural State Forest Engineering University. 336 p. (In Russian with English summary).

Usoltsev, V.A. 2016b. Biological productivity of forest-forming species in Eurasia's climatic gradients (as related to supporting decision-making processes in forest management) [Biologicheskaya produktivnost' lesoobrazuyushchikh porod v klimaticheskikh gradientakh Evrazii (k menedzhmentu biosfernykh funktsiy lesov)]. Ekaterinburg, Ural State Forest Engineering University. 384 p. (In Russian with English summary).

Uri, V., Lõhmus, K., Ostonen, I. Tullus, H., Lastik, R., & Vildo, M. 2007. Biomass production, foliar and root characteristics and nutrient accumulation in young silver birch (*Betula pendula* Roth.) stand growing on abandoned agricultural land. Eur. J. For. Res. 126(4): 495–506. doi:10.1007/s10342-007-0171-9

Uria-Diez, J. & Pommerening, A. 2017. Crown plasticity in Scots pine (*Pinus sylvestris* L.) as a strategy of adaptation to competition and environmental factors. Ecol. Model. 356: 117–126. doi:10.1016/j.ecolmodel.2017.03.018

Varik, M., Kukumägi, M., Aosaar, J., Becker, H., Ostonen, I., Lõhmus, K. & Uri, V. 2015. Carbon budgets in fertile silver birch (*Betula pendula* Roth) chronosequence stands. Ecol. Eng. 77: 284–296. doi:10.1016/j.ecoleng.2015.01.041

Walter, J.-M.N. & Himmler, C.G. 1996. Spatial heterogeneity of a Scots pine canopy: an assessment by hemispherical photographs. Can. J. For. Res. 26: 1610–1619. doi:10.1139/x26-181

Widlowski, J.-L., Verstraete, M., Pinty, B., & Gobron, N. 2003. Allometric relationships of selected European tree species. EC Joint Research Centre, Technical Report EUR 20855 EN, Ispra, Italy. 61 p.

Wu, H., Sharp, P.J., Walker, J., & Penridge, L.K. 1985. Ecological field theory: a spatial analysis of resource interference among plants. Ecol. Model. 29: 215–243. doi:10.1016/0304-3800(85)90054-7

Xiao, C.-W., Yuste, J.C., Janssens, I.A., Roskams, P., Nachtergale, L., Carrara, A., Sanchez, B.Y., & Ceulemans, R. 2003. Above- and belowground biomass and net primary production in a 73-year-old Scots pine forest. Tree Physiol. 23: 505–516. doi:10.1093/treephys/23.8.505

Yarmishko, V.T. 1999. Vertical structure of aboveground biomass profiles of *Pinus sylvestris* L. at northern range limit under atmospheric pollution [Vertikal'no-fraktsionnaya struktura nadzemnoy fitomassy *Pinus sylvestris* L. na severnom predele rasprostraneniya v usloviyakh atmosfernogo zagryazneniya]. Rastitel'nye resursy 35(1): 3–13. (In Russian).

Yeatts, D. (2012). Tree Shape and Branch Structure: Mathematical Models. Mathematical and Computational Forestry & Natural-Resource Sciences (MCFNS), 4(1), Pages: 2–15 (14). Retrieved from http://mcfns.net/index.php/Journal/-article/view/MCFNS.4%3A2

Appendixes: Electronic Supplemental Material

A Estimation of the Model Parameters.

The coefficients of Equations (1–4) (Thorpe et al., 2010) were estimated with published data (Pugachevskiy, 1992; Rautiainen, Stenberg, 2005; Tahvanainen, Forss, 2008; Tselniker et al., 1999; Usoltsev, 2013b, 2016; Widlowski et al., 2003) with the least squares method in R statistical software (R Core Team, 2014). The goodness-of-fit of the model was estimated with R^2 and slope for predicted vs. observed values and normalized root mean square deviation (NRMSD) (Table 3, Figure 7).

To refine the parameters of equations describing vertical distribution of biomass inside the crown, we started with the initial values as presented in (Tahvanainen, Forss, 2008). Since the source dataset used in (Tahvanainen, Forss, 2008) is not presented in the paper, we used the original values of parameters and dispersion to generate the virtual dataset. The additional data on biomass distribution (Bobkova et al., 2000; Gspaltl et al., 2013; Gulbe et al., 1983; Mäkelä, Vanninen, 2001; Usoltsev, 2013a; Yarmishko, 1999) was added to this dataset, and then the Equation (5) was fitted to this new dataset with the least squares method using R statistical software (R Core Team, 2014). Given the small number of added data points, in comparison to already presented in original dataset (150 vs. 12305 for spruce, 144 vs. 10301 for pine, and 108 vs. 7125 for birch) and due to the fact that the relationship reported in additional sources had the same pattern as those presented in (Tahvanainen, Forss, 2008), the parameters did not changed remarkably (see Appendix C below), in comparison to the original ones, except the parameters of foliage mass distribution in birch that were not reported in the original study and were therefore estimated only with the new sources. The goodness-of-fit of the model (R^2 and slope for predicted vs. observed, NRMSD) was estimated for new data points only (Tab. 3, Fig. 8).

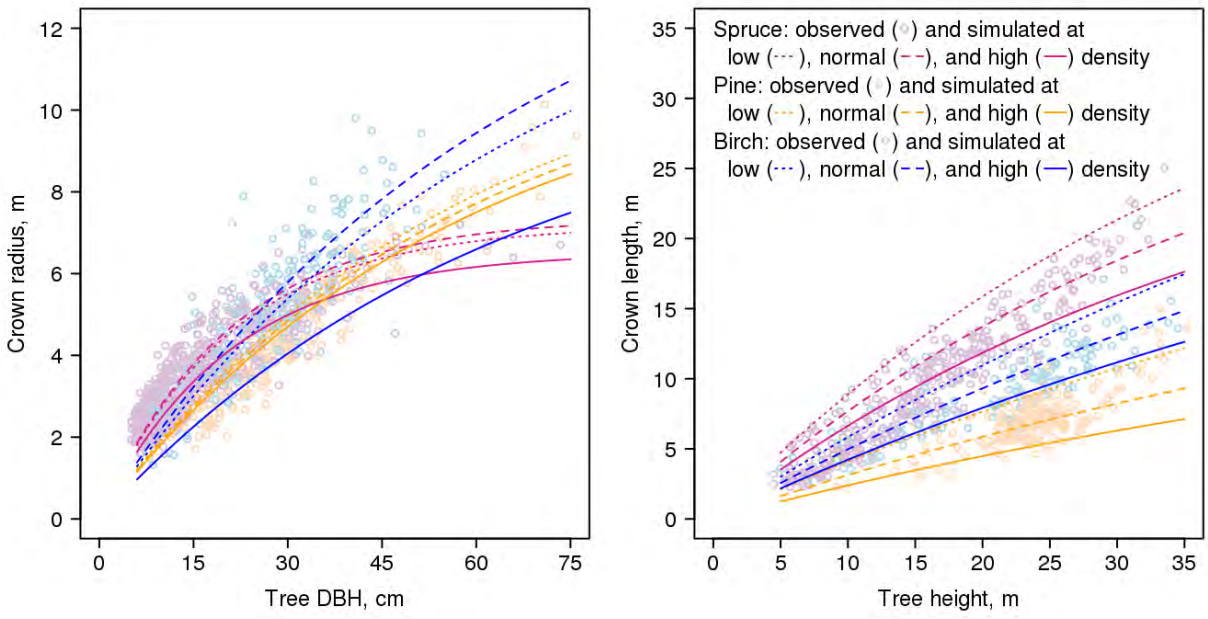

Figure 7: The relationship between tree stem dimensions and crown size: experimental data and predicted curves. Since the local stand density around the focal tree is also used as predictor (which cannot be illustrated with 2D-diagram), three type of curves based on fixed values of NCI (2000 for low, 5000 for medium, and 8000 for high density) were used to depict the influence of competition gradient.

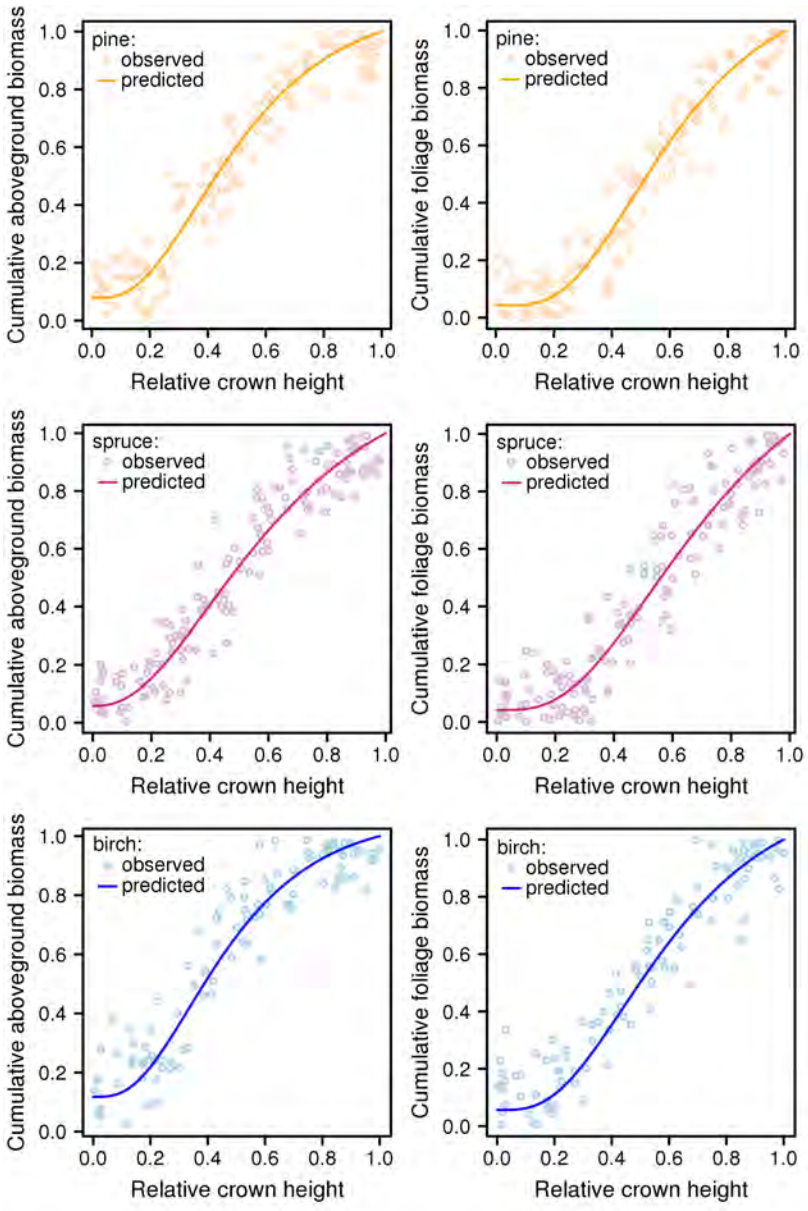

Figure 8: The relationship between relative crown height (ratio between specified height from crown base and total length of crown) and cumulative portion of biomass: predicted curves and experimental data.

Table 3: Goodness-of-fit of equations for crown size and biomass distribution inside the crown.

	Crown Radius			Crown Length			Biomass			Foliage		
	Pine	Spruce	Birch	Pine	Spruce	Birch	Pine	Spruce	Birch	Pine	Spruce	Birch
NRSMD	0.594	0.883	0.896	0.658	0.613	0.861	0.086	0.086	0.094	0.087	0.097	0.095
R^2	0.988	0.977	0.859	0.968	0.966	0.976	0.982	0.980	0.982	0.977	0.969	0.976
Slope	1.041	1.029	1.005	0.907	1.088	1.027	1.019	0.997	0.997	1.012	0.991	0.983

B Calculation of the Above-Canopy PAR

The density of the PAR flux above the canopy at a clear sky is calculated as follows (Peng et al., 2002):

$$PAR_0 = I_0 \cdot \phi_{PAR} \cdot \sin\beta_{sun} \cdot e^{\frac{-K_{atm}}{\sin\beta_{sun}}} \cdot c_{hs} \cdot c_{MJ}, \quad (12)$$

where I_0 is the solar constant (equal to 1367 $\mathrm{W \cdot m^{-2}}$), φ_{PAR} is the portion of photosynthetically active radiation (equal to 0.47), K_{atm} is the coefficient of atmospheric absorption of solar radiation (equal to 0.15), β_{sun} is the solar elevation angle, c_{hs} is the conversion factor from second to hourly time step (equal to 3600 $\mathrm{s \cdot hr^{-1}}$), c_{MJ} is the conversion factor from $\mathrm{W \cdot m^{-2}}$ to $\mathrm{MJ \cdot m^{-2} \cdot s^{-1}}$ (equal to 10^{-6}) - (McCree, 1981).

The solar elevation angle β_{sun} is the function of latitude, season of year, and time of day; it is calculated as follows:

$$\sin\beta_{sun} = \sin\lambda \cdot \sin\delta + \cos\lambda \cdot \cos\delta \cdot \cos\left(\frac{2 \cdot \pi}{24} \cdot (t_h - 12)\right) \quad (13)$$

where λ is latitude, δ is solar declination, t_h is time of day (hour), and 24 is the number of hours per day.

Solar declination is calculated as a function of t_d - ordinal number of the given day of year, starting from January 1st:

$$\delta = -23.45 \cdot \cos\left(\frac{360}{365} \cdot (t_d + 10)\right) \quad (14)$$

where 23.45 is the angle of the Earth axis inclination relatively to the normal to ecliptic plane (degrees of arc); 360 is the full circle (degrees of arc); 365 is the number of days per year, and expression $t_d + 10$) defines the number of days since the winter solstice.

C Parameters of the Model

Table 4 lists estimated on empirical data species-specific coefficients of the model and associated with them summary statistics.

D Validation of Crown Size With the Regression-Based Equivalence Test.

We used the regression-based equivalence test as proposed in (Robinson et al., 2005) with bootstrap (10000 replications) to additionally validate the model in terms of calculation of crown dimensions. The null hypothesis is that there is dissimilarity between the observed and simulated values. According to the technique, the procedure was as follows:

1. At each replication n pairs of values were randomly selected from the original sample (where n is the number of values in the original sample), allowing each pair to be selected more than once.
2. The simulated values were shifted by the subtraction of mean simulated value from them: $y_{sh} = y_i - y_{\mathrm{mean}}$.
3. The regions of equivalence were established: I_0 for the shifted intercept as $y_{\mathrm{mean}} \pm 0.1$, and I_1 for slope as 1.0 ± 0.1.
4. The linear regression model was fitted to the obtained dataset using the simulated values as a predictor (independent) variable and the observed (experimental) values as a response (dependent) variable.
5. The coverage probability was estimated by counting whether or not the value β_0 (calculated on the basis of the intercept value of the above linear regression and its standard error) is within the interval of equivalence for the intercept (I_0), and whether or not the value β_1 (calculated on the basis of the slope value of the above linear regression and its standard error) is within the interval of equivalence for the slope value (I_1).

After the above-described operations were completed, the proportion of times when the bootstrap estimations of intercept and slope were within the corresponding regions of equivalence was calculated. The above tests (for intercept and slope) was based on $\alpha = 0.05$. However, since these are independent, the overall value of α at joint interpretation is $1 - (1 - 0.05)^2 = 0.0975$. To correct this, the value for each test should be calculated as follows: $\alpha = 1 - \sqrt{1 - 0.05} = 0.02532$.

Therefore, if the proportion of either $\beta_0 \subset I_0$ or $\beta_1 \subset I_1$ is greater than $1 - (2 \times 0.02532) = 0.9494$, the null hypothesis of dissimilarity between the observed and simulated values should be rejected with $\alpha = 0.05$ (Robinson et al., 2005). The summary of tests is presented in Table 5. The tests showed that all proportions were greater than 0.9494 that means no dissimilarity between simulated and measured values.

E Validation of the Model in Terms of Above-Canopy Solar Radiation.

The amount of incoming solar radiation above the canopy is the important part of the ecosystem model because it allows to take into account the geographic differences. Since data on direct measurements of PAR are relatively sparse, in comparison to data on total solar radiation, and Equation (12) is actually an expression

Table 4: Coefficients of Equations (1–9) for different tree species (±SE, where applicable). Subscript $_{CR}$ denotes coefficients for crown width, subscript $_{CL}$ represents coefficients for crown length. Subscript $_{BM}$ denotes coefficients for total aboveground biomass, excluding the stem (i.e., foliage and branches), $_{LV}$ represents the coefficients for foliage biomass separately. The SE is not presented for χ_{BM} and χ_{LV}, since these parameters are scaling factors, and for ρ since the only one value for each species was found in literature.

Parameter	Species		
	Pine	Spruce	Birch
α	3.788±0.289	2.519±0.103	2.254±0.0717
ε	1.283±0.147	1.448±0.129	1.386±0.173
γ	-0.0838 ± 0.00876	-0.0471 ± 0.00492	-0.0642 ± 0.00771
μ	0.724±0.0378	0.296±0.0155	0.682±0.0965
ν_{CR}	12.484±0.477	7.428±0.0812	16.027±0.0784
ν_{CL}	38.167±1.795	45.420±3.707	52.571±2.021
η_{CR}	-0.0174 ± 0.00165	-0.0482 ± 0.00227	-0.0154 ± 0.00248
η_{CL}	-0.0137 ± 0.00148	-0.0243 ± 0.00193	-0.0142 ± 0.000374
κ_{CR}	$-0.00000946 \pm 0.0000000804$	$-0.00000162 \pm 0.00000458$	$-0.00000478 \pm 0.00000236$
κ_{CL}	$-0.0000892 \pm 0.000000265$	$-0.0000486 \pm 0.00000506$	$-0.0000539 \pm 0.00000271$
σ_{BM}	0.0788±0.00257	0.0589±0.0589	0.119±0.00431
σ_{LV}	0.0427±0.00721	0.0417±0.00717	0.0570±0.00982
τ_{BM}	1.030±0.00583	1.185±0.0113	0.961±0.00851
τ_{LV}	1.137±0.0263	1.314±0.0518	1.139±0.0414
ψ_{BM}	-3.596 ± 0.0538	-2.589 ± 0.0539	-3.907 ± 0.0938
ψ_{LV}	-3.430 ± 0.185	-2.622 ± 0.188	-3.146 ± 0.234
ω_{BM}	3.667±0.0906	2.765±0.0683	3.659±0.0152
ω_{LV}	4.987±0.452	3.962±0.358	3.979±0.361
χ_{BM}	0.991	0.986	0.989
χ_{LV}	0.993	0.984	0.987
S_{LV}	9.520±0.190	7.290±0.0879	17.500±0.932
ρ	0.570	0.640	0.520
L_{min}	0.340±0.0272	0.015±0.00321	0.290±0.0126

Table 5: Summary of the regression-based equivalence tests.

Parameter	n	$\beta_0 \subset I_0$	$\beta_1 \subset I_1$
crown width, spruce	595	1.0000	0.9964
crown width, pine	244	1.0000	1.0000
crown width, birch	271	1.0000	1.0000
crown length, spruce	328	1.0000	0.9925
crown length, pine	197	1.0000	0.9841
crown length, birch	137	1.0000	0.9831

for the calculation of total solar radiation at a clear sky, multiplied by the reducing coefficient φ_{PAR} (portion of photosynthetically active radiation), this equation can be rewritten as follows (i.e., omitting the φ_{PAR} parameter):

$$SOL_0 = I_0 \cdot \sin\beta_{sun} \cdot e^{\frac{-K_{atm}}{\sin\beta_{sun}}} \cdot c_{hs} \cdot c_{MJ} \qquad (15)$$

where SOL_0 is the total solar radiation at a clear sky. The total solar radiation, taking into account cloudiness (SOL), can be calculated similarly to Equation (7):

$$SOL = SOL_0 \cdot (1 - 0.8 \cdot C_{cld}) \qquad (16)$$

The results of calculations with Equations (15) and (16) were then compared to the measured total incoming solar radiation (Lebedev et al., 1979; Anonymous, 1987–2001); the results are shown in Figure 9. The measured values are long-term averages of monthly solar radiation, measured by meteorological stations. For European Russia, the measured monthly sums for the clear sky conditions are also available. The observed jittering in the distribution of points along the latitudinal

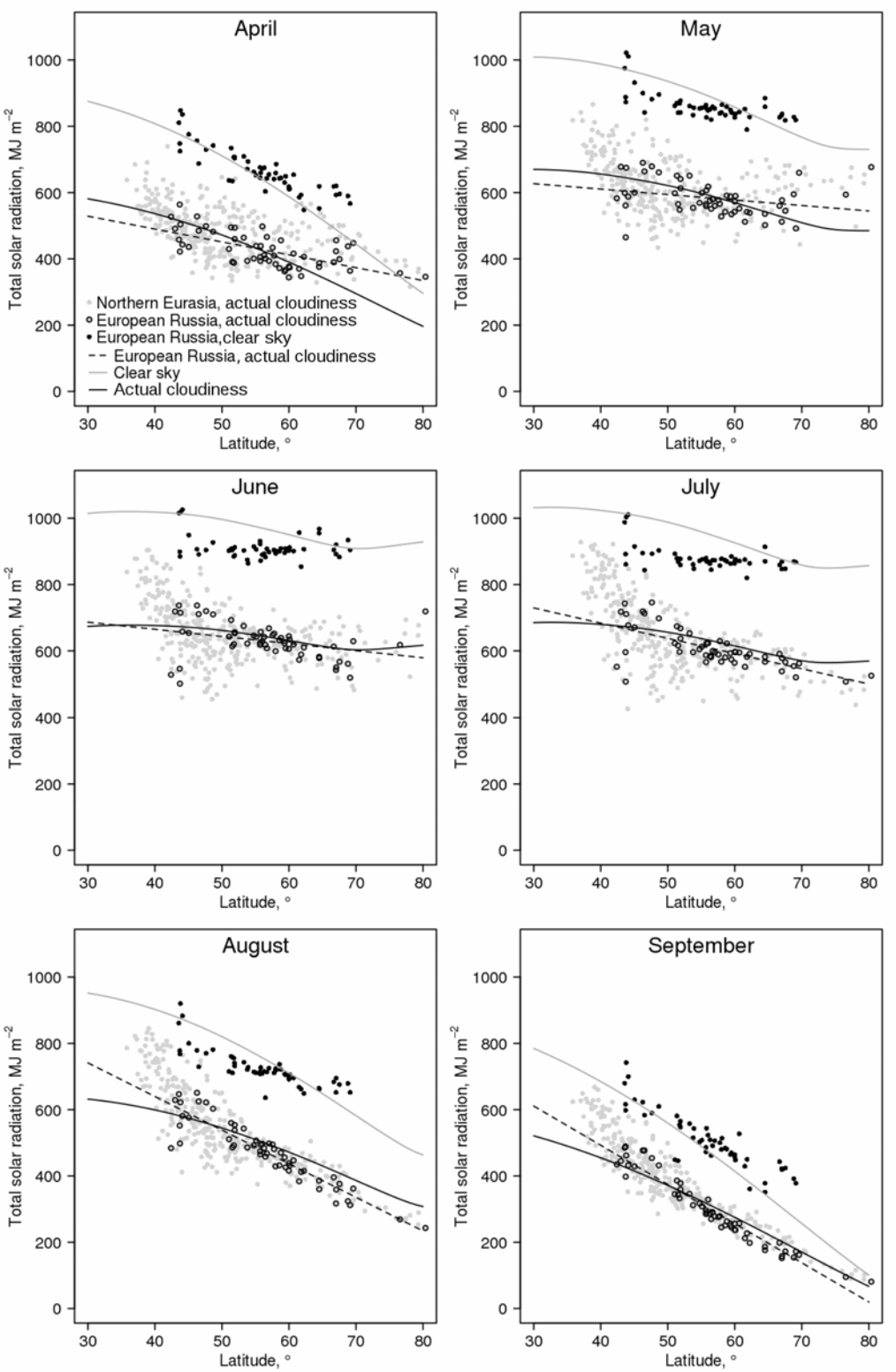

Figure 9: Measured data (points) on total solar radiation at actual cloudiness for Northern Eurasia and separately for European Russia, linear approximation for the latter (dashed line), total solar radiation at clear sky (only data from European Russia are available), and simulated total solar radiation at cloudy and clear sky (solid lines).

Table 6: Analysis of sensitivity of the model to variations in its parameters.

Parameter	CVMC	LRC
	Parameters affecting crown size	
α	0.0496	−0.190
ε	0.0113	0.0826
γ	0.00315	−0.0259
μ	0.00559	−0.0432
ν_{CR}	**0.202**	**0.701**
ν_{CL}	0.0802	0.228
η_{CR}	0.135	−0.411
η_{CL}	0.0705	−0.201
κ_{CR}	0.00397	0.0311
κ_{CL}	0.00162	0.0119
	Parameters affecting spatial distribution of biomass inside crown	
σ_{BM}	0.00000402	0.00112
σ_{LV}	0.00000284	0.00370
τ_{BM}	0.0000388	0.00431
τ_{LV}	0.0000281	0.0125
ψ_{BM}	0.0000629	−0.00618
ψ_{LV}	0.0000660	−0.0249
ω_{BM}	0.0000326	−0.00507
ω_{LV}	0.0000349	−0.0208
A_N	0.00296	0.00229
A_E	0.00566	0.0176
A_S	**0.00931**	**0.0580**
A_W	0.00505	0.0157
	Parameters affecting overlap of crowns	
E_{max}	0.00559	−0.0432
E_{min}	0.00559	−0.0432
E_{corr}	**0.00576**	**0.0447**
	Parameters affecting absorption and interception of PAR	
S_{LV}	0.000122	0.0103
C_{cld}	**0.0737**	**−0.213**
P_{dir}	0.0178	−0.0332
R_{mrn}	0.0202	0.0609
R_{aft}	0.0603	0.183
ρ	0.000122	0.0103
	Basic input characteristics of stand	
DBH	**0.192**	**0.464**
H	0.0200	0.00824
N_{tr}	0.00985	−0.0615
Intercept		−2.403
R^2		0.856
Residual standard error		0.378

gradient (deviation from the functional relationship) can be explained by differences in elevation and atmospheric transmittance (and also by different monthly cloudiness in the case of radiation at a cloudy sky) for different observation points.

Obviously, the simulated incoming radiation with regard to cloudiness (i.e., actual amount of radiation above the canopy), calculated according to the above Equation, is dependent on the value of the cloud factor C_{cld}, and the best fit to the measured data for the European part was observed when the value of the cloud factor was set at 0.42 (Figure 9). However, some improvements can be introduced to the model after collecting additional data: (i) taking into account the elevation; (ii) assuming the regional values of the cloud factor C_{cld} and the coefficient of atmospheric absorption of solar radiation K_{atm}; and (iii) taking into account seasonal changes in the distance between Sun and Earth.

F Sensitivity Analysis.

Table 6 contains the sensitivity analysis of the model parameters.

In the Table 6, CVMC is the coefficient of variation (standard deviation divided by mean) for OAT runs in Monte-Carlo mode; LRC is the standardized linear regression coefficients of the sensitivity analysis as proposed in (Saltelli, Annoni, 2010). All values of LRC are significant ($p<0.001$). The most influential parameters (with maximal absolute value) in each group are marked by bold font (separately for both approaches).